ECO-FRIENDLY SYNTHESIS OF SILVER NANOPARTICLES BY USING GREEN METHOD: IMPROVED INTERACTION AND APPLICATION *IN VITRO* AND *IN VIVO*.

Q. S. Atwan N. H. Hayder
Researcher Prof.
Department of Biotechnology, College of Science, University of Baghdad, Baghdad, Iraq.

ABSTRACT

The present study was aimed to biosynthesis of silver nanoparticles by using rhaminolipid produced from local isolate *Pseudomonas aeruginosa* as reducing and stabilizing agent. Silver nanoparticles (AgNPs) synthesized by green method have shown several applications such as biomedical, anticancer, bio sensing, catalysis etc. Characterization study of purified bioemulsifier using thin layer chromatography (TLC) was demonstrated that the biosurfactant contains mono, and di- rhamnolipid with *Rf* values of 0.86 and 0.36 respectively. Optimization results of biosynthesis silver nanoparticles were revealed that an increasing in intensity of Surface Plasmon Resonance (SPR) bands of nanoparticles with shifting at wavelength (400 nm). Also optimum synthesis of AgNPs was at pH 5, Temperature 40℃, reaction time 5 minutes with concentration of rhaminolipid as reducing agents (2×10^{-3}w/v) and Silver ion concentration (6×10^{-3} mol/L). The result of X-ray diffraction was indicated that the size of silver nanoparticles observed was 38 nm and show relatively stable peak at -23.2 mV. Finally, the minimum inhibitory concentration of Ag NPs against human pathogenic bacteria obtained at concentration (1mg/ml) for both gram negative and gram-positive bacteria. The results of anti-inflammatory effects of Ag NPs obviously, cleared that the infection of test animals treated with AgNPs were completely healed after 6 days of treatment, while the animals treated with fucidin (as control) not exhibited any healing in the infection.

Keywords: silver nanoparticles, optimization, characterization, antimicrobial activity, anti-inflammatory, biosurfactant.

تصنيع دقائق الفضة النانوية الصديقة للبيئة باستخدام طريقه الخضراء: تحسين التفاعل وتطبيقه في المختبر وفي جسم الكائن الحي

قصي سعدون عطوان ناظم حسن حيدر
باحث أستاذ
قسم التقنيات الأحيائية، كليه العلوم، جامعة بغداد، بغداد، العراق.

المستخلص:

هدفت الدراسة الحالية الى تصنيع الدقائق النانوية باستخدام الرامينولبد المنتج من العزلة المحلية لبكتريا الزائفة الزنجارية كعامل مختزل ومثبت لدقائق الفضة النانوية. حيث تمتلك دقائق الفضة النانوية المصنعة بالطريقة الخضراء عده استعمالات طبية حياتية مثل مضادة للخلايا السرطانية، التحسس الحيوي، محفزات وغيرها. أظهرت نتائج توصيف المستحلب الحياتي باستخدام كروموتوغرافيا لأغشية الرقيقة بان الرامينولبد مكون من نوعين هما احادي وثنائي الرامينولبد حيث تمتلك كل منهما قيمه *Rf* (الحركة النسبية) بمقدار 0.86 و0.36 على الترتيب. تم دراسة الظروف المثلى لتصنيع دقائق الفضة النانوية حيث بينت النتائج ازدياد في حزمه بلازما لدقائق الفضة النانوية مع تحركها عند الطول الموجي(400 nm) ، كذلك درست الظروف المثلى لإنتاج الدقائق الفضة النانوية حيث تبين الرقم الهيدروجيني الأمثل للإنتاج هو 5 ودرجة الحرارة 40℃، خلال زمن تفاعل مساوي الى 5 دقائق بتركيز الرامينولبد (كعامل مختزل) (2×10^{-3}w/v) وتركيز ايون الفضة (6×10^{-3} mol/L). أظهرت نتائج حيود الأشعة السينية بان حجم دقائق الفضة النانوية الناتجة 38 nmبثباتيه النسبية عند (−23.2 mV). كذلك أوضحت النتائج ان دقائق الفضة النانوية تمتلك فعالية علاجية عالية ضد الالتهاب بالممرضات البكتيرية (الموجبة والسالبة لصبغة الغرام) عند تركيز (1mg/ml) حيث ظهرت بشكل واضح بعد تعافي الحيوانات المصابة بعد معاملتها بدقائق الفضة النانوية بعد 6 أيام من المعالجة مقارنة بالحيوانات المعاملة باستخدام المضاد الحيوي الفيوسيدين (عامل سيطرة) لم تظهر أي استجابة للشفاء.

الكلمات المفتاحية: دقائق الفضة النانوية، تحسين، توصيف، فعالية مضادة للبكتريا، مضاد للالتهاب، المستحلب الحياتي

***Received:11/1/2019, Accepted:3/4/2019**

INTRODUCTION

Metal nanoparticles have a key role in many applications as they show superior physicochemical properties (optical, catalytic activity, magnetic, Electronic, and antibacterial properties) due to their significantly small size and very high surface area, This case distinguishes nanoscale and opens its horizons in many application, where it can penetrate and damage the walls of microorganisms. In addition, binds with any material on the surface of the Nano molecule easily to produce new results (15). Silver nanoparticles (AgNPs), finds their utility in various applications such as biomedical, healthcare, pharmaceutical, cosmetics, environmental, catalysis, hardware, water treatment, and energy (44). AgNPs can be manufactured by several methods such as chemical reduction, electrochemical techniques, photochemical reduction, sonochemical, microwave and biological methods (green method) (47). The chemical reduction method for synthesis silver nanoparticles is still expensive and employ hazardous organic solvents and toxic reducing agents (14). So Preferred use green method to prepare silver nanoparticles as less toxic, less harmful, safe and low cost. In green synthesis, using extracts of natural products is a promising innovation that would beat the obstructions in chemical methods indicated so far. Different biological processes has been reported for the synthesis of metal nanoparticles using various plant extract, honey, bacteria, and fungi (1, 9). Biosurfactant isolate from bacteria have amphipathic in nature with both hydrophilic and hydrophobic moieties, and exhibit surface-active properties. Many microorganisms like bacteria, fungi, yeasts, and algae are good sources of biosurfactant and have several advantages over their chemical counterparts; they are less toxic and biodegradable (25). Biosurfactant have a wide range of applications including microbial enhanced oil recovery (MEOR), bioremediation, medicine, pharmaceuticals, gene delivery system, cosmetics, food, and beverages (31). Recognizing the importance of developing eco-friendly methods for the synthesis of biologically active nanoparticles, scientists have recently started looking into research relating to the synthesis of metallic nanoparticles with the additional use of biosurfactant as capping agents (17). Biosurfactant are now mediating new developments in the field of Nanotechnology. It was observed that biosurfactant produced by microorganisms could play a very important role in aggregation and stabilization process (18). Biosurfactant use has therefore now emerged as a green alternative for enhancing both nanoparticles synthesis (reducing agent) and stabilization (stabilizing agent). One of the modes of action is through adsorbing onto nanoparticles, surface stabilizing the nanoparticles and prevent of formation subsequent aggregation (7). This study was aimed; the purified rhamnolipid from *Pseudomonas aeruginosa* was used to biosynthesize of silver nanoparticles as reducing and stabilizing agent (23). As well as the potential application of the synthesized nanoparticles in *vitro* as antibacterial activity against human pathogenic bacteria was studied and in *vivo* as anti-inflammatory activity of AgNPs

MATERIALS AND METHODS

Bacterial isolate and culture media

The bacterial isolate used in the present study was previously isolated from petroleum-contaminated soil and exhibited high biosurfactant produced and obtained from biotechnology department. The bacterial isolate was identify using the VITEK 2 System.

Media and fermentation conditions for biosurfactant production

Fermentation media Preparation based on Niladevi-Prema Design (24). Medium prepared by mixing components such as NaCl: 0.1 g/l, $FeSO_4$: 0.01g/l, $ZnSO_4$: 0.009 g/l, $MgSO_4$: 0.002 g/l, $CaCO_3$: 0.02 g/l, $CuSO_4$: 0.001 g/l, KH_2PO_4: 0.5 g/l and K_2HPO_4: 1g/l and 1% KNO_3 as nitrogen source and 1% of olive oil as carbon sources .The pH was adjusted to 7.0, then sterilized by autoclaving at 121℃ for 15min. After sterilization, the medium left to cool and inoculated 1% of the selected bacteria isolate (1×10^8 CFU, OD=0.5) and incubated in a shaker incubator at 30℃ at 120 rpm for 96h.

Extraction and purification of biosurfactant

Acid precipitation method was used to extraction of biosurfactant (BS). After end of incubation time the culture were centrifugation at 10000 rpm for 15 min, the pellets were discard and the supernatant was used for biosurfactant extraction. 2N of HCl solution was used to acidify the supernatant containing BS, until pH 2. The mixture was then incubated for 24 hrs at 4℃. The precipitate formed was collected by separation funnel by adding chloroform and methanol (2:1) for partially purified, precipitate was then dried, in oven at 60℃ and after 24 hrs of drying process, a brown color precipitate was obtained (36). For further purification of biosurfactant, 50 grams of silica gel (mesh 60-120) were placed in column ($26\times3.3cm^2$) after activation by heating 60℃ for 1.5 h, and a slurry of the silica gel was made by rinsing it in chloroform. A gram of partial purified biosurfactant after dissolved in 5 ml of chloroform was poured on the slurry, and the chloroform continuously added until all neutral lipids were eluted. Three volumes of chloroform/methanol (250, 200 and 100) were added to the column at ratios (50:3), (50:5) and (50:50), respectively. The first and second addition eluted mono-rhamnolipoid (60 ml/hr.), while the last addition for elution of di-rhamnolipid. The surface tension of eluted volumes was measured, and then allowed to evaporation for removing of solvents. The separated biosurfactant were characterized by TLC to insure the full separation of both types of glycolipid (38).

Surface-active properties and determination of critical micelle concentration (CMC)

The surface tension of the culture supernatant was measured by the Wilhelmy plate method with tensiometer (QBZY-2Processor Tensiometer; China).The critical micelle concentration (CMC) was measured by plotting the concentration of the surfactant as a function of surface tension, and the CMC was taken as the point the slope of the curve abruptly changed (37). The critical micelle concentration (CMC) corresponds to the concentration of a surface-active compound at which surface becomes fully loaded with surfactant molecules and above which micelles are formed. Therefore, measurement of surface tension could be used to find CMC. Purified rhaminolipid (RLs) were dissolved in deionized water at concentrations ranging from 100 to 1.5 mg/L. The accuracy of the measurements was controlled by the surface tension measurements of water before each set of measurements. The CMC and the surface tension at the CMC were determined from the breakpoint in the surface tension (6).

Synthesis of silver nanoparticles

Silver nitrate ($AgNO_3$, 99%) (Aldrich/Germany) was used in the preparation of the silver nanoparticles. Silver nanoparticles were synthesized according to a method described by Martinez-Gutierrez *et al*., (22) with modification. Method of synthesis are done by two solutions:

Solution (A) is prepared as follows: 0.02 gm (0.1 mmol) of $AgNO_3$ were dispersed by ultrasonication in 20 ml deionized water (DI) for 2 minutes. The interaction and production of nanoparticles need for reducing agent and stabilizer to prevent aggregation. In addition, solution (B) prepared by dissolving 0.002gm (w/v) of rhaminolipid in 20 ml DI water and dispersed by ultra-sonication for 2 minutes. Its acts as capping stabilizer and reducing agent. Solutions (A and B) are mixed by magnetic stirrer and exposed to the direct sunlight for about 5 min at pH 5. The solution contains silver nanoparticles, was separated and concentrated by centrifugation at 10,000 rpm for 15 min and washed twice by DI water and also precipitated by centrifugation at 10,000 rpm for 15 min. then dried in the oven at 60℃ for 30 minutes to obtain a brownish black powder, and kept in dark vial for further characterization and applications. The biosynthesis of silver nanoparticles by this method was optimized with different parameters such as pH, temperature, time of reaction and concentrations for $AgNO_3$ and biosurfactant,

Optimized conditions for nanoparticles synthesis

 # Effect of pH

The AgNPs solutions (20 ml of 0.1mmol of $AgNO_3$ and 20 ml of 0.002 gm w/v of biosurfactant) were prepared with different pH; the pH reaction was maintained at (5, 7, 9 and 11), and adjusted by using HCL (0.1 N)

and NaOH (0.1N). The mixture was exposed to direct sunlight for 5 minutes. The absorbance of the resulting solutions was measured using Uv-vis spectrophotometer (SHIMADZU 1800 double beam region (1901100) nm, Japan).

Effect of temperature

Silver nanoparticles (AgNPs) solutions were prepared at different temperature (30, 40, 50 and 60℃), using stirring hot plate to get suitable temperature. The absorbance of the resulting solutions was measured using Uv-vis spectrophotometer.

Effect of reaction time

The reaction time of synthesized nanoparticles was optimized using different time intervals. The reaction time was monitored at (1, 5, 10 and 15 min). The absorbance of the resulting solutions was measured using Uv-vis spectrophotometer.

Effect of silver ion concentration

The effect of silver nitrate ($AgNO_3$) concentration on biosynthesis of silver nanoparticles was evaluated using 20 ml of different concentrations, included 0.04 mM (2×10^{-3} mol/L), 0.08 mM (4×10^{-3} mol/L), 0.1 mM (6×10^{-3} mol/L) and 0.2 mM (8×10^{-3} mol/L) each concentration was mixed with 20 ml of 0.002 gm (w/v) of biosurfactant separately. The reaction was maintained in pH 5 at 40℃ under direct sunlight. The absorbance of the resulting solutions was measured using UV-vis spectrophotometer.

Effect of biosurfactant concentration

Biosurfactant (rhaminolipid) concentration is one of the most important factors affecting on biosynthesis of silver nanoparticles. Similarly, the concentration of biosurfactant and silver nitrate was optimized with the increasing concentration of biosurfactant, 20 ml of different concentrations 0.001, 0.002, 0.004 and 0.006 gm (w/v), were mixed with 20 ml of optimized concentration of $AgNO_3$ from previous step in pH 5 at 40℃. The absorbance of the resulting solutions was measured using UV-vis spectrophotometer.

Antibacterial test (*in vitro*)

The antibacterial activity of AgNPs were investigated using gram negative bacteria (*Escherichia coli*) and gram positive bacteria (*Staphylococcus aureus*) that obtain from department of biotechnology, university of Bagdad .The minimal inhibition concentration (MIC) of AgNPs for each test microorganism was determined by applying agar well diffusion technique (2). The biosurfactant and synthetic AgNPs from (Hongwu, China) used as negative control in a same concentration of green AgNPs that used in all experiment. Approximately, 25 mL of sterilized Müller Hinton agar medium was poured into sterilized Petri dishes and allowed to solidify at room temperature. The overnight growth test organisms were transferred and spread over the agar medium using a sterile cotton swab separately, wells were made. After that, different concentrations of green AgNPs (0.1, 0.25, 0.5, 1, 5, 10 mg/ml), and negative control (biosurfactant and synthetic AgNPs) were added as same the concentration of green AgNPs to the wells. The AgNPs inoculated plates were incubated at 37 °C for 24 h. After incubation, the zone of inhibition around the well was measured (33).

Anti-inflammatory activity of AgNPS

Preparation of AgNPs paste

The paste was prepared from the following gradients: 25g of Vaseline to collect components and protect the mixture from drying, 25mg of methyl paraben (0.1%) as preservative, 1.25ml of glycerol (5%) as a moisturizer and to prevent of the skin from dry, rough, scaly, itchy and irritations. All the above components were mixed with synthesis AgNPS at concentration of MIC. These ingredients are mixed and kept in the refrigerator until use.

Anti-inflammatory activity in-*vivo*

Laboratory animal (Rabbit) were used for in-*vivo* anti-inflammatory test, the animal divided in to two groups: A control and B the test. Both groups of Rabbit are injected with 1ml from overnight activated clinical pathogen *Staphylococcus aureus* OD=0.5 under the skin for infection. The animal left for 48h for appearance the pus, cracking and finely inflammation of skin. There after the inflammation test was carried out by wiping the test animals with synthesized AgNPs ointment daily until the healing of inflammation. Control animal also treated using Fucidin ointment (LEO pharma, Ireland) instead of synthesized Ag NPs ointment.

RESULTS AND DISCUSSION

Identification of the biosurfactant producing isolate

In the current study the selected bacterial isolate for biosurfactant production was identified by using VITEK2 compact system based on biochemical testes. The selected isolate for biosurfactant production was in 97% similarity with *Pseudomonas aeruginosa*.

Production of biosurfactant

The maximum biosurfactant concentration that produced from isolate was 14 g/L occurred at 96 h of incubation, when the cells reached their early stationary phase. It was observed that the crude biosurfactant showed good emulsification activity (EI24 value) reached 70% with lowering the surface tension of the water from 72 to 26 mN/m Fig(1). Bazsefidpar *et al.*, (5) observed maximum rhaminolipid production in a lab-scale fermenter as batch culture reached to 22.5 g/L after 120 h. Also Noh *et al*., (26) obtained 23.6 g/L of rahminolipid from culture *P. aeruginosa* USM-AR2 using submerged batch fermentation conditions.

Characterization of biosurfactant

The structural analysis of biosurfactants produced by P. aeruginosa Q1. One of the important test for the detection of presence of glycolipid nature of biosurfactan is Molisch's test (α – Naphthol), based on the dehydration of the carbohydrate by sulfuric acid to produce an aldehyde, which condenses with two molecules of phenol resulting in a red- or purple-colored compound (45). From the results, it was shown that the biosurfactant contains carbohydrate residues. The phenol – sulphuric acid reaction tested for lipid content of biosurfactants. The biosurfactant gave the positive results with phenol – sulphuric acid reaction. This means that the biosurfactant obtained in this study have lipid content. Thin layer chromatography suggested the obtained of biosurfactant from *P. aeruginosa* was composed of rhamnolipid. The extracted product was separated on TLC plates with a carrier solvent of (chloroform Methanol: acetic acid, 65:15:2 by volume). Similar results observed by (45), when they analyzed commercially available purified rahmnolipid produced by *Pseudomonas aeruginosa* Q1 on TLC plates. They observed two characteristic spots. The lower (high molecular weights) spot consist of di-rhamnolipid (*Rf* = 0.36), while the higher (low molecular weight) spot consisted mono- rhamnolipids (*Rf* = 0.84) Fig (2). Santos-Guerra *et al*., (12), also observed the active compounds production by *P. aeruginosa* on TLC, with the *Rf* values are 0.4 and 0.8 for di- and mon- rhamnolipid respectively.

Critical Micelle Concentration (CMC) of rhaminolipid

The results of CMC of produced biosurfactant are illustrated in (Fig.3). The results indicated that the CMC of the RL produced by P. aeruginosa Q1was 50 mg/l and reduced the surface tension of water to 26 mN/m similar the result in EI-Sheshtawy (10).

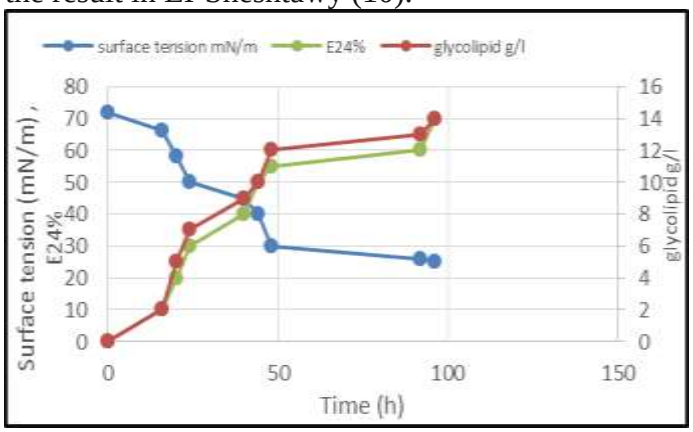

Fig1. Production of biosurfactant during time

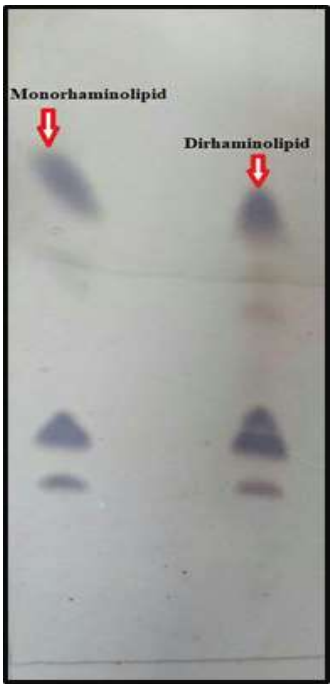

Fig 2. Thin layer chromatography of purified Rhaminolipids

'

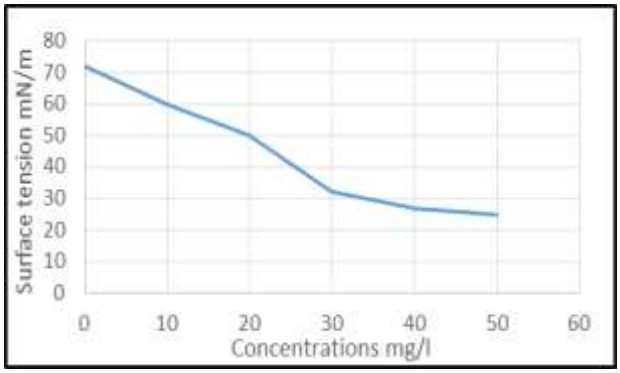

Fig 3. Critical Micelle Concentration (CMC) of Rhaminolipid.

UV–Visible analysis of AgNPs

Noble metal nanoparticles (plasmonic) are distinguished from other nanoparticles such as semiconductor quantum dots, polymeric, and magnetic nanoparticles by their unique surface plasmon resonance (SPR). Optical absorption spectra of AgNPs is dominated by SPR which illustrates a shift toward the brown or yellow end depends on particle size, state of aggregation, shape, and the surrounding dielectric medium (21). The synthesis of AgNPs was monitored by color change and UV–Vis spectroscopy. The formation of AgNPs was confirmed by changing in the solution color from colorless to yellow brown. Optimum condition for AgNPS synthesis to achieve the optimum conditions for the synthesis of AgNPs, different factors were studied in this procedure such as concentration of silver nitrate and Rhaminolipid, stirring time, pH, and temperature. In each step of the synthesis ideal nanoparticles, samples are examined by using the UV–Vis spectroscopy and the application of the nano product as antibacterial agent against pathogenic bacteria were studied in order to determine all the optimum conditions in the production of silver nanoparticles.

Effect of Ph

pH have a great influence in formation of nanoparticle and have the capability in affecting on compounds that used in mixture by a charge change. Green synthesis of silver nanoparticles has demonstrated their stabilization by natural material using rhaminolipid at concentration (2×10^{-3} w/v) as reducing and stabilizing agent that reduce $AgNO_3$ (6×10^{-3} mol/L). The results observed in (Fig.4) that the optimum pH was 5 for synthesis of Ag NPs at wavelength (415 nm). These results were in agreement with Velgosová *et al*., (43). The antimicrobial activity of silver nanoparticles at different pH values were illustrated in Table 1, the result showed that dimeter of inhibition zones decrease with increasing pH. Higher inhibition obtained at pH 5. Increase pH towards alkalinity give high yield comparing to less yield in acidic conditions (28). At high pH, the nanoparticles started to agglomeration and particles suffer from aggregation (29), which led to decrease the inhibition zones.

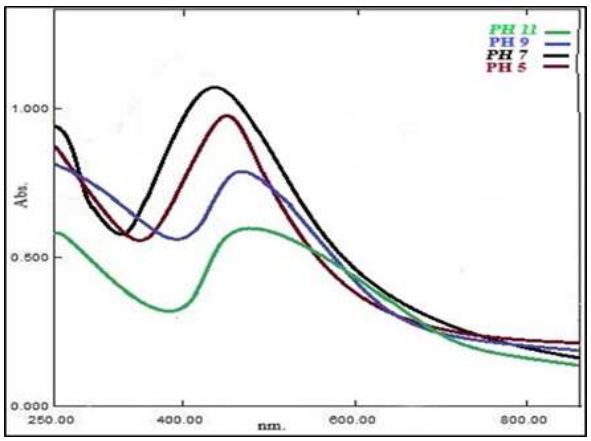

Fig 4. UV–Vis spectroscopy of AgNPs: The effect of pH of Ag NPs formation

Table 1. Effect of different pH on Ag NPs synthesis and inhibition zone of Ag NPs against pathogenic bacteria

NO.	pH	UV–Vis peak Nm	Zone Dimeter (mm)	
			Staphylococcus aureus	*Escherichia coli*
1	5	415	17	14
2	7	409	13	11
3	9	450	≤10	≤10
4	11	463	≤10	≤10

Effect of temperature Temperature elevation can increase the reaction rate and efficiency of synthesis. Most studies are carried out at room temperature, as it is the simplest and natural way of synthesizing the nanoparticle. As the temperature, increases the time of reaction decreases and 95% conversion into nanoparticle within short time (20). When the mixture exposed to temperature of sunlight and by using magnetic stirrer work as control

of interaction movement and regulation temperature in same time. The mixture was exposed for different temperature (30, 40, 50 and 60 ℃) with an ideal conditions for the interaction that was obtained from the results of previous steps. The result showed that 40℃ was the optimum temperature for synthesis of Ag NPs at wavelength (408 nm) (Table 2). This temperature have narrow peak and give high inhibition zone against pathogenic bacteria (8). These results indicate that the factor of temperature not only influences on the reaction rate but also affects the morphologies of silver NPs and SPR as shown in (Fig.5). Similar results were recorded by Lee *et al*., (19). Increasing temperature lead to anxiety in the reaction and increase the probability of aggregation, therefore the particles size were increased with increasing temperature. The increase of temperature values of NPs the decrease the inhibition zones of pathogenic bacteria (13).

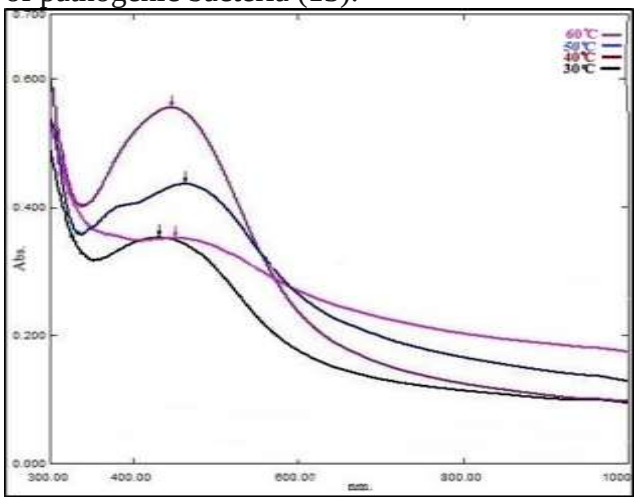

Fig 5. UV–Vis spectroscopy of AgNPs: Effect of temperatures

Table 2. Effect of different Temperature on AgNPS synthesis and inhibition zone of AgNPS against pathogenic bacteria

No.	Temperature	UV–Vis peak Nm	Zone Dimeter (mm)	
			Staphylococcus aureus	*Escherichia coli*
1	30 ℃	405	12	11
2	40 ℃	408	19	14
3	50 ℃	420	14	12
4	60 ℃	413	10	≤10

Effect of time on reaction

The time is one of the important parameter that effecting directly on biosynthesis of nanoparticles. The reduction reaction for formation of nanoparticles started when reducing agents were add immediately to silver nitrate solution, which is noted by the color change from light to brown. However, it is seen that the particle size increases with increasing time and stabilize at a particular time (15). The mixture exposed to different period time for synthesis AgNPs (1, 5, 10 and 15 min) taking into account the results of optimal conditions in the previous steps. Maximum synthesis of Ag NPs observed at five minute in direct sunlight (Fig 6 and Table 3) at wavelength (427 nm). As the time of reaction increased the size of nanoparticles also increased and affect negatively to synthesis of NPs. The results of current study were in accordance to the previous study of Shaban *et al*., (35). The result also showed that the higher inhibition zones of silver nanoparticles against on *S. aureus* and *E. coli* were observed within five minutes of reaction, reached to 19 and 15 mm respectively. In the current study increasing the time of reaction led to reduce the diameter of inhibition zone around well, therefore the time of reaction was maintained at five minutes for remaining experiments

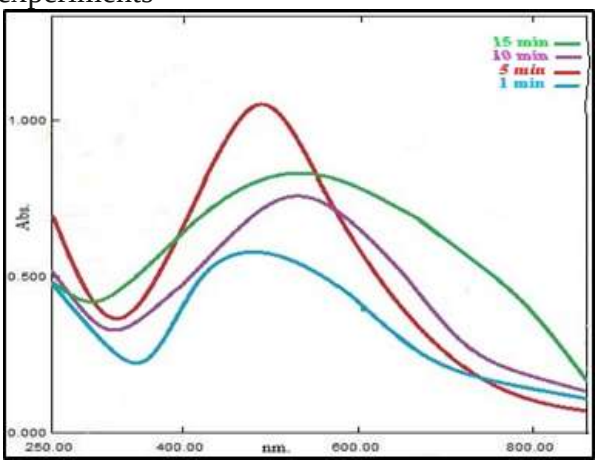

Fig 6. UV–Vis spectroscopy of AgNPs: Effect of Time on Reaction

to avoid the aggregation of AgNPs. The results were in agreement with the study of Yusof *et al*., (46).

Table 3. Effect of different period's time on AgNPS synthesis and inhibition zone of AgNPS against pathogenic bacteria

No.	Time (min)	UV–Vis peak Nm	Zone Dimeter (mm)	
			Staphylococcus aureus	*Escherichia coli*
1	1	418	14	12
2	5	427	19	15
3	10	477	11	10
4	15	490	≤10	≤10

Effect of silver ion concentration

Silver nitrate ($AgNO_3$) is most frequently used as a source of silver ions. The concentration of silver nitrate solution used also has an effect on silver nanoparticle formation. At first neutral silver atoms collide with each other, forming stable nuclei and production of the nanoparticle occurs until all metal ions are consumed so must be finding suitable reducing agent and prevention of nanoparticles agglomeration by an addition of protecting agents to prevent the aggregation via their interactions with small particle (40). Different concentration of silver nitrate (2, 4, 6 and 8) $\times 10^{-3}$ mol/L were added to a solutions of rhaminolipid at concentration (2×10^{-3} w/v) in previous optimum conditions (pH 5, temperature 40℃ and reaction time 5 minutes). Results showed that the best concentration of silver ion was 6×10^{-3} mol/L for synthesis of nanoparticles was at wavelength (410 nm) (Fig 7). The position of an absorption band depends on the silver nitrate concentration. In general, as the particles become larger the plasmon peak shifts to longer wavelengths and broadens (39) so finding concentration-selected showed have narrow peak. The antibacterial activity of silver nanoparticles performed at different silver nitrate concentrations. AgNPs synthesized displayed antibacterial activity at all the silver nitrate concentrations against both S. aureus and E. coli (Table 4). The concentration 6×10^{-3} mol/L of silver nitrate give high inhibition zone. The results showed decrease in diameter of inhibition zones as the concentration of silver nitrate increased more than 6×10-3 mol/L. This can be correlated to the increase in particle size as the concentration of silver nitrate increased during synthesis (27). The result of inhibition zones for synthesized Ag NPs were in agreement with the finding of Augustine *et al*., (3), they observed that the increase the concentration of Ag NPs from 1 to 5 mM has been reduced the inhibition zones of test pathogens.

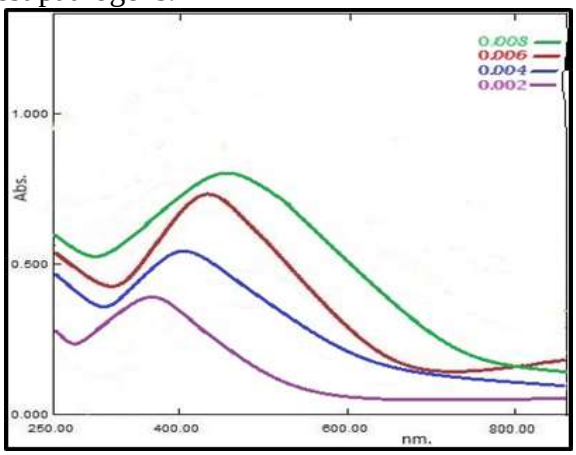

Fig 7. UV–Vis spectroscopy of AgNPs: Effect Silver ion Concentration

Table 4. Effect of different concentration of silver nitrate on AgNPS synthesis and the inhibition zone of AgNPS against pathogenic bacteria

No.	Concentration mol/L	UV–Vis peak Nm	Zone	Dimeter (mm)
			Staphylococcus aureus	*Escherichia coli*
1	2×10^{-3}	396	12	10
2	4×10^{-3}	406	14	11
3	6×10^{-3}	410	18	14
4	8×10^{-3}	425	11	≤10

Effect of rhaminolipid concentration

One of the importance of developing eco-friendly biologically material relating to the synthesis of metallic nanoparticles is the additional of biosurfactants as capping agents (30). Concentration of rhaminolipid added to mixture effect on formation of silver nanoparticles, its act as reducing and stabilizing agent in same time (17). The effect of partial purified rhaminolipid concentration on the synthesis of AgNPs was studied by adding different concentrations of rhaminolipid (1, 2, 4 and 6) $\times 10^{-3}$ mol/L (w/v) to $AgNO_3$ solution 6×10^{-3} mol/L at previous

optimum conditions. The result obviously showed that the concentration of rhaminolipid (2×10^{-3} w/v) was optimum for the synthesis AgNPS, at wavelength (420), which low wavelength absorption related to small particle size formation of Ag NPs (Table 5 and Fig.8). Also high inhibition zone of synthesized nanoparticles against pathogenic bacteria observed at the same concentration of rhaminolipid and relatively low surfactant concentration was required to produce small droplets of AgNPs. This result were similar with that found by Bai (4). The intensity of the SPR bands increased and shifted to wavelength (500 nm) when the concentration of the rhaminolipid increased from (4 to 6×10^{-3} w/v), (Fig.8). This reduces in the intensity of the SPR band perhaps because of the aggregation of nanoparticles, which is in concurrence with previous study of Velammal *et al*. (42).

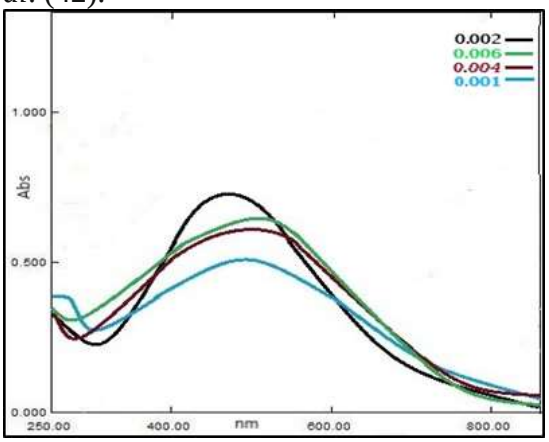

Fig 8. UV–Vis spectroscopy of AgNPs: Effect of Rhaminolipid concentration.

Table5. Effect of different concentration of Rhaminolipid on Ag NPS synthesis and the inhibition zone of Ag NPS against pathogenic bacteria

No.	Concentration w/v	UV–Vis peak nm	Zone Dimeter (mm)	
			Staphylococcus aureus	*Escherichia coli*
1	1×10^{-3}	455	12	10
2	2×10^{-3}	420	19	13
3	4×10^{-3}	490	12	11
4	6×10^{-3}	500	≤10	10

FT-IR analysis

FT-IR measurements were recorded to identify the major functional groups on the rhaminolipid to examine their possible involvement in the production and capping of AgNPs. FT-IR spectrum of rhaminolipid aqueous extract shows different bands positioned at 3423, 3004, 2925, 2856, 1741, 1622, 1461, 1178, 1066 and 730 cm^{-1} (Fig 9). The presence of bands at 3423 and 3386 cm^{-1} could be related to stretching of (OH) and 3004 cm^{-1} related to (C-H)(Aromatic). The bands positioned at 2925 and 2856 cm^{-1} may be due to (C-H) stretching of alkanes. The band at 1741 cm^{-1} related to (C=O) carboxyl group (Aldehyde). A sharp intense band observed at 1622 cm^{-1} can be due to the stretching vibration of alkene (C=C) group (Silverstein *et al*.,1981). The observed band at 1461 cm^{-1} may be bending deformation (C-H) Alkane and band at 1178 cm^{-1} is (C-N) Amine. The observed band at 1066 cm^{-1} related to (C-O) Alkyl Halide and band at 730 cm^{-1} may be related to (C-Cl). The FT-IR spectrum also analyze for synthesis of $AgNO_3$ (Fig 10). The observed band at 1382 cm^{-1} related to stretching (N-O). The results of FT-IR spectrum for AgNPs aqueous solution also observed the bands at 2925, 2856, 1741 and 1622 cm^{-1} are the same bands and positions that found in the examination of partial purified rhaminolipid. These means that rhaminolipid made up as capping agent for synthesis AgNPs. Also the band of Ag NPs at 1382 cm^{-1} shifted to another position and appeared at band 1367 cm^{-1}(Fig 11), this is another conformation to the synthesis AgNPs

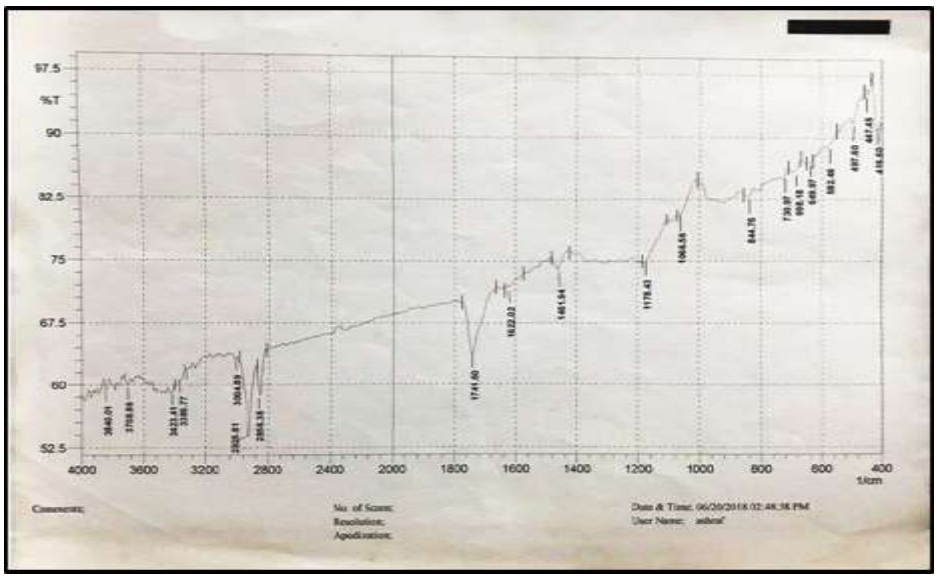

Fig 9. The Fourier transform infrared (FT-IR) spectroscopy measurement of Rhaminolipid

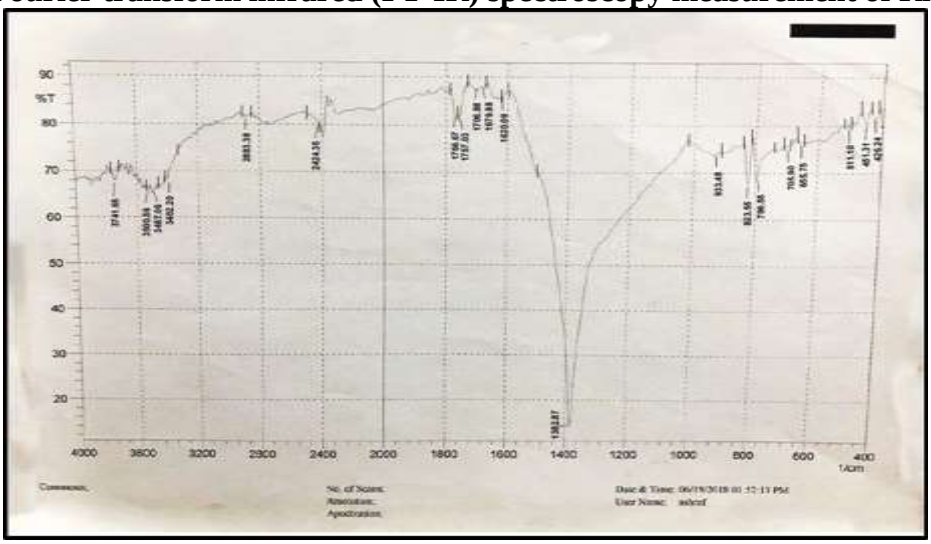

Fig 10. The Fourier transform infrared (FT-IR) spectroscopy measurement of $AgNO_3$

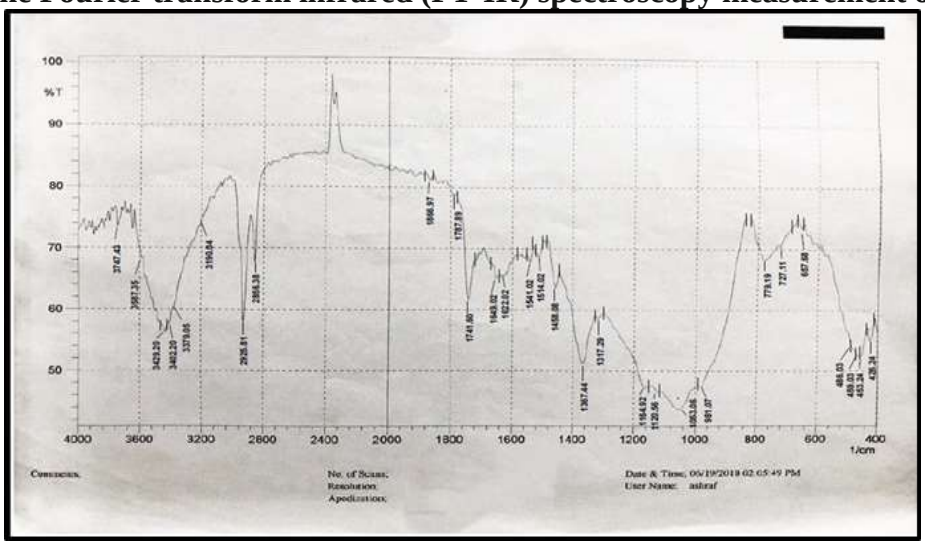

Fig 11.The Fourier transform infrared (FT-IR) spectroscopy measurement of AgNPs.

XRD analysis

The XRD patterns (Fig.12) show the distinctive diffraction peaks of AgNPs at 2θ =29.60°, 35.44°, 38.07°, 43.39°, 64.42° and 77.39°, These peaks were well matched with standard diffraction data of AgNPs (JCPDS file no. 040783) and attributed to the (495), (5508), (1814), (352), (403) and (209). Silver with a lattice parameter of a = 4.0862 Å which were in good agreement with reference of the

face-centered cubic (fcc) crystal lattice of metallic silver. The size of the AgNPs calculated by Debye-Scherrer equation ($D = 0.94\lambda/d \cos\theta$).The size of AgNPs was 38 nm.

Atomic force microscopy

The surface morphology of the Ag NPs was studied by atomic force microscopy and give 2D and 3D topological for AgNPs (Fig 13). AFM images shows the synthesized Ag NPs are in spherical shape. The size also estimated by AFM in a range 53 nm (Fig 14).

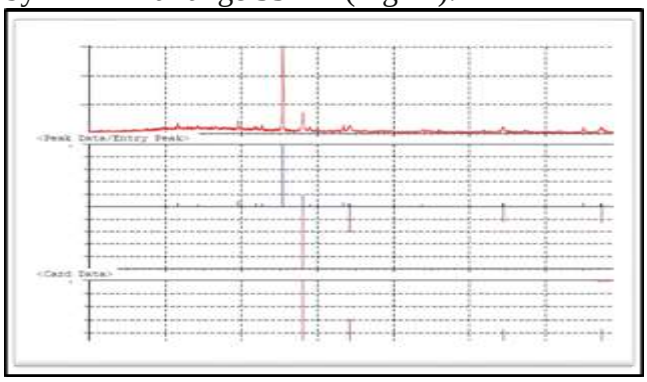

Fig 12. X-ray Diffraction (XRD) for AgNPS.

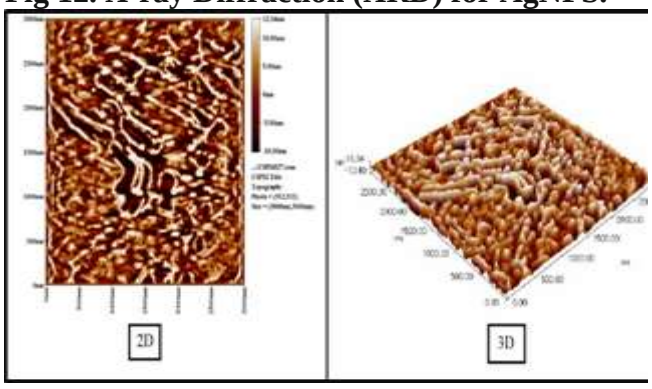

Fig 13. Atomic Force Microscopy of AgNPs illustrate

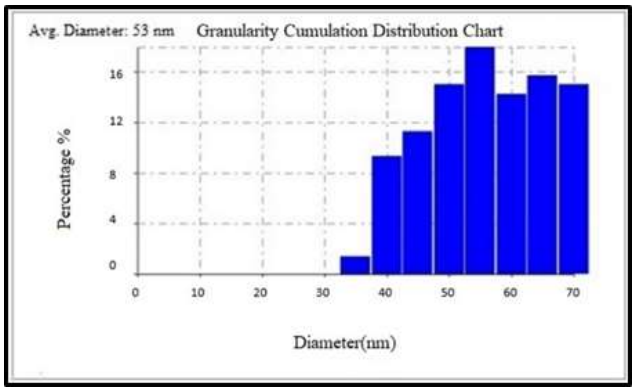

Fig 14. Estimate size of AgNPs by AFM. 2D and 3D topological

Zeta potential measurement

Zeta potential is a basic parameter for classification of stability in aqueous Ag NPs suspensions. As shown in (Fig.15) the Ag NPs obtain have a negative zeta potential value .The Zeta potential measurements of the biosynthesized Ag NPs show a sharp peak at -23.2 mV indicative of that the surface of the nanoparticles is negatively charged. Generally, the zeta potential of the nanoparticles should be either highest than +30 mV or lower than -30 mV (34).

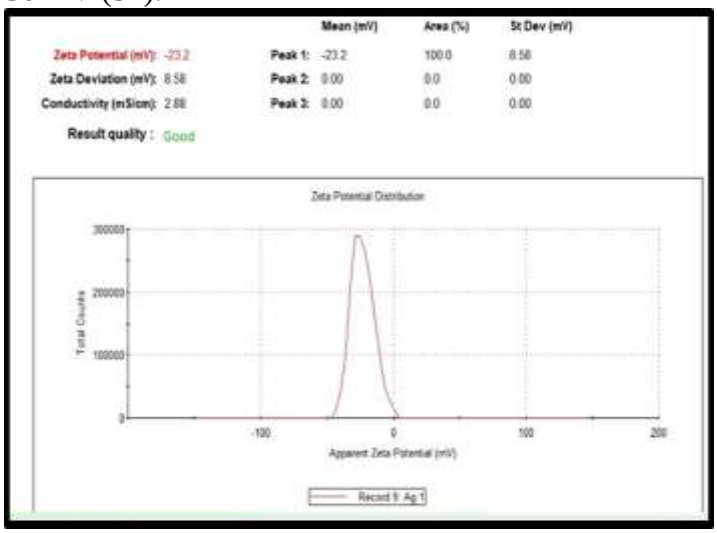

Fig 15. Zeta potential measurement of AgNPs

Antibacterial susceptibility teste

The results of antibacterial activity of AgNPs were shown in Fig. 16 and 17. The antibacterial activity was found to be straightly reliant on the concentration of the AgNPs. Table 6 show that the maximum inhibition zones of *S. aureus* and *E.coli* were 21 and 18 mm respectively at concentration 10 mg/ml of Ag NPs, while the minimum inhibition zones was found at concentration of 1 mg/ml of Ag NPs. The dissimilarity in diameter of inhibition, may be due to different interactions of AgNPs with the microorganism and due to the susceptibility of bacteria used in the current study. The main mechanism of AgNPs toxicity probably related to the attachment of AgNPs to the negatively charged bacterial cell wall, where they can disrupt its shape and permeability of the plasma membrane (27). In addition, all studies had confirmed that silver ions released from nanoparticle surface contribute to their toxicity. AgNPs invade the bacterial cells and inhibit many cellular enzymes especially the respiratory chain enzymes via adhering to sulfur containing macromolecules leading to protein inhibition and death (48). However, many studies to date have used high concentrations of silver nanoparticles and found (1ppm) that could be

considered environmentally and healthy relevant (41).

Table 6. Antibacterial susceptibility test

No.	AgNPs concentration mg/ml	Zone Dimeter (mm)	
		S. aureus	*E.coli*
1	0.1	Nil	Nil
2	0.25	Nil	Nil
3	0.5	Nil	Nil
4	1	12	10
5	5	19	16
6	10	21	18

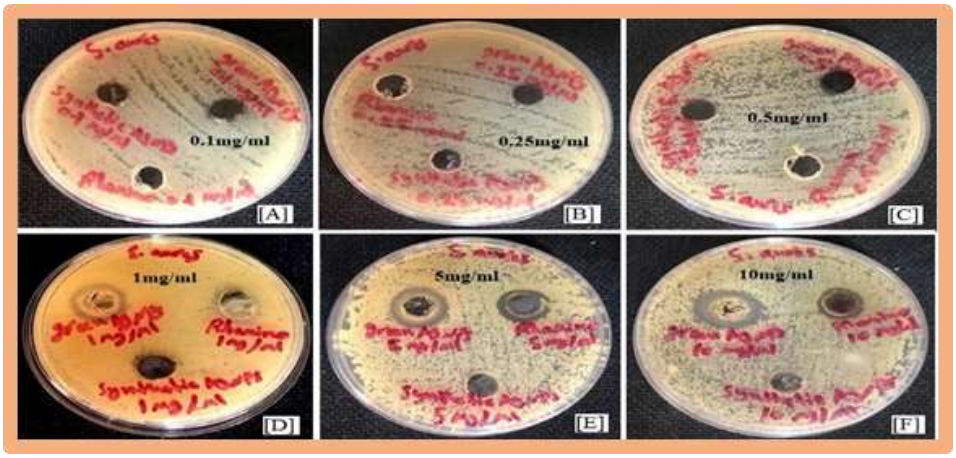

Fig 16. Antimicrobial susceptibility test of AgNPS against *S. aureus* at different concentration.

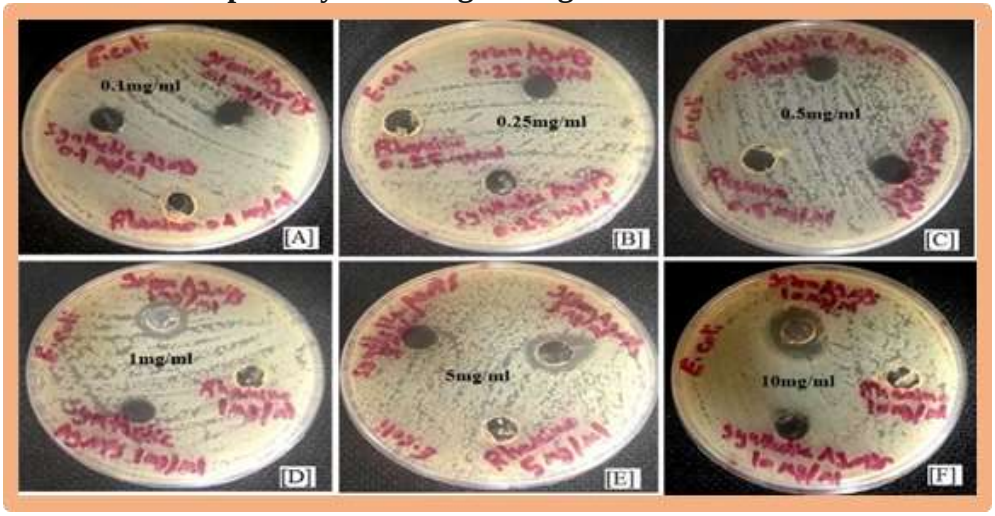

Fig 17. Antimicrobial susceptibility test of AgNPS against *E.coli* at different concentration.

Anti-inflammatory activity of AgNPs

The biological activity of Ag NPs as anti-inflammatory effect *in vivo* was investigated using laboratory animals. After injection the skin of animals with pathogenic bacteria (*staph*) in two different places, the infection was appeared after 48 h. Thereafter the treatment of infected animals was started by wiping daily with synthesized AgNPs as well as fucidin ointments as control. The results in Fig 18 (A1, B1) obviously cleared that the infections of test animals treated with Ag NPs were completely healed after 6 days of treatment, while the animals treated with fucidin Fig 18 (A2, B2) not exhibited any healing in the infection. Additionally, it was concluded that AgNPs could induce cell death of pathogenic bacteria. Moreover, it was concluded that NPs of small size (38nm) primarily induced cell death of pathogenic bacteria, probably by attachment of AgNPs to the cell wall of bacteria, where they can disrupt its shape and permeability of the plasma membrane as mentioned (11).

Fig 18. The healing of infection Rabbit by AgNPs ointment (A1 and B1) and Fucidin (A2 and B2) after 6 days of treatment.

Green synthesis of nanoparticles makes use of environmental friendly non-toxic and safe reagent. rhaminolupid production from *P. aeruginosa* and extraction by acid precipitation method by using 2N of HCl solution and purified by silica gel and examination on TLC. Purified Rhaminolipid was characterization by FT-IR and using for synthesis AgNPs by green method. Biosynthesis of silver nanoparticles presence by sunlight was optimization to obtained best synthesis. The suitable concentration of reducing agent (Rhaminolipid) was (2×10^{-3} mol/L). The best concentration of $AgNO_3$ was 6×10^{-3} mol/, Temperature of reaction was 40℃, pH of reaction was 5 and Time suitable for reaction was five minutes. AgNPs by green method was characterization by UV–visible Spectroscopy where a final SPR band at 420nm.The crystallinity determined by X-ray Diffraction (XRD) Silver with a lattice parameter of a = 4.0862 Å which were in good agreement with reference of the (FCC). The size was estimated 38 nm and surface morphology of the Ag NPs by atomic force microscopy (AFM) and give 3D topological for AgNPs. The FT-IR measurements were recorded to identify the major functional groups for purified Rhaminolipid and to identifying the functional groups of Rhaminolipid act as reducing agent for AgNPs. The stability of synthesized AgNPs was measured by Zeta potential measurement and show relatively stable when peak at -23.2 mV. Finally silver nanoparticles application in vitro as antimicrobial activity against human pathogenic bacteria both gram negative such as (*E.coli*) and gram positive such as (*S. aureus*) show good activity and minimum inhibitory concentration also counting were 1mg/ml for both bacteria. In *vivo* application by ointment of skin to treatment *Staph* infection that cause pus, inflammation and cracking on rabbit skin in 6 days of treatment of infection cream of silver nanoparticles was kill the bacteria and the skin returned to its normal state.

REFERENCES

1. Ahmed, S., M. Ahmad, B. L. Swami and S. Ikram 2016. A review on plants extract mediated synthesis of silver nanoparticles for antimicrobial applications: a green expertise. Journal of advanced research, 7(1), 17-28

2. Ashokkumar, S., S. Ravi, V. Kathiravan, and S. Velmurugan. 2015. "RETRACTED: Synthesis of silver nanoparticles using A. indicum leaf extract and their antibacterial activity: 34-39

3. Augustine, R., N. Kalarikkal and S. Thomas 2014. A facile and rapid method for the black pepper leaf mediated green synthesis of silver nanoparticles and the antimicrobial study. Applied Nanoscience, 4(7), 809-818

4. Bai L. and DJ. McClements 2016 Formation and stabilization of nanoemulsions using biosurfactant: Rhaminolipids. J Colloid Interface Sci.; 479: 71-79

5. Bazsefidpar, S., B. Mokhtarani, R. Panahi and H. Hajfarajollah 2019. Overproduction of rhamnolipid by fed-batch cultivation of *Pseudomonas aeruginosa* in a lab-scale fermenter under tight DO control. Biodegradation, 1-11

6. Bonilla, M., C. Olivaro, M. Corona, A. Vazquez, and M. Soubes 2005. Production and characterization of a new bioemulsifier from *Pseudomonas putida* ML2. J. Appl. Microbiol. 98, 456–463. doi: 10.1111/j.1365-2672.2004.02480.x

7. Chen Y, KY Lie and J. Li 2009. Size controlled synthesis of Co nanoparticles by combination of organic solvent and surfactant. Appl Surf Sci, 255, 4039–4044

8. Daizy, P. 2010. Green synthesis of gold and silver nanoparticles using Hibiscus rosa sinensis. Phys. E, 42, 1417–1424

9. Dong, C., C. Cao, X. Zhang, Y. Zhan, X. Wang, X. Yang, and B. Yuan 2017. Wolfberry fruit (Lycium barbarum) extract mediated novel route for the green synthesis of silver nanoparticles. Optik-International Journal for Light and Electron Optics, 130, 162-170

10. El-Sheshtawy, H. S., and M. M. Doheim 2014. Selection of *Pseudomonas aeruginosa* for biosurfactant production and studies of its antimicrobial activity. Egyptian Journal of Petroleum, 23(1), 1-6

11. Franci, G., A. Falanga, S. Galdiero, L. Palomba, M. Rai, G. Morelli and M. Galdiero 2015. Silver nanoparticles as potential antibacterial agents. Molecules, 20(5), 8856-8874

12. Guerra-Santos, L.; O. Kappel, and A. Fiechter, 1984. *Pseudomonas aeruginosa* biosurfactant production in continuous culture with glucose as carbon source. Appl. Environ. Microbiol. 18(2): 301-305

13. Gupta, S. K., M. Talati and P. K. Jha, 2008. Shape and size dependent melting point temperature of nanoparticles. In Materials Science Forum 570:132-137. Trans Tech Publications

14. Gurusamy, V., R. Krishnamoorthy, B. Gopal and V. Veeraravagan 2017. Systematic investigation on hydrazine hydrate assisted reduction of silver nanoparticles and its antibacterial properties. Inorganic and Nano-Metal Chemistry, 47(5), 761-767

15. Indana, M. K., B. R. Gangapuram, R. Dadigala, R. Bandi and V. Guttena 2016. A novel green synthesis and characterization of silver nanoparticles using gum tragacanth and evaluation of their potential catalytic reduction activities with methylene blue and Congo red dyes. Journal of Analytical Science and Technology, 7(1), 19

16. Joy, S., T. Butalia, S. Sharma and P. K. Rahman 2017. Biosurfactant producing bacteria from hydrocarbon contaminated environment. In Biodegradation and Bioconversion of Hydrocarbons pp: 259-305. Springer, Singapore

17. Kiran GS, A. Sabu and J. Selvin 2010. Synthesis of silver nanoparticles by glycolipid biosurfactant produced from marine Brevibacterium casei MSA19. J Biotechnol, 148, 221–225

18. Kvitek, L.; A. Panacek, J. Soukupova, M. Kolar, R. Vecerova, R. Prucek, M. Holecova and R. Zboril 2008. Effect of surfactants and polymers on stability and antibacterial activity of silver nanoparticles (NPs). J. Phys. Chem. C. 112, 5825–5834

19. Lee, S. W., S. H. Chang, Y. S. Lai, C. C. Lin, C. M. Tsai, Y. C. Lee and C. L. Huang 2014. Effect of temperature on the growth of silver nanoparticles using Plasmon-mediated method under the irradiation of green LEDs. Materials, 7(12), 7781-7798

20. Li, S., Y. Shen, A. Xie, X. Yu, L. Qiu, L. Zhang and Q. Zhang 2007. Green synthesis of silver nanoparticles using *Capsicum annuum* L. extract. Green Chemistry, 9(8), 852-858

21. Mahmudin, L., E. Suharyadi, A. B. S. Utomo and K. Abraha 2015. Optical properties of silver nanoparticles for surface plasmon resonance (SPR)-based biosensor applications. Journal of Modern Physics, 6(08), 1071

22. Martinez-Gutierrez, F., P. L. Olive, A. Banuelos, E. Orrantia, N. Nino, E. M. Sanchez and Y. Av-Gay 2010. Synthesis, characterization, and evaluation of antimicrobial and cytotoxic effect of silver and titanium nanoparticles. Nanomedicine: Nanotechnology, Biology and Medicine, 6(5), 681-688

23. Mulligan, C. N., R. N. Yong and B. F. Gibbs 2001. Heavy metal removal from

sediments by biosurfactants. Journal of hazardous materials, 85(1-2), 111-125

24. Niladevi, K.N. and P. Prema, 2005. Mangrove actinomycetes as the source of ligninolytic enzymes. Actinomycetol. 19, 40–47

25. Nitschke, M., S. G. Costa and J. Contiero 2005. Rhamnolipid surfactants: an update on the general aspects of these remarkable biomolecules. Biotechnology Progress, 21(6), 1593-1600

26. Noh, Nur and Md. Asshifa 2012. Rhamnolipid produced by Pseudomonas aeruginosa USM-AR2 facilitates crude oil distillation." The Journal of general and applied microbiology58.2: 153-161

27. Panáček, A., L. Kvitek, R. Prucek, M. Kolář, R. Večeřová, N. Pizúrová and R. Zbořil 2006. Silver colloid nanoparticles: synthesis, characterization, and their antibacterial activity. The Journal of Physical Chemistry B, 110(33), 16248-16253

28. Prathna, T. C., N. Chandrasekaran, A. M. Raichur and A.Mukherjee 2011. Biomimetic synthesis of silver nanoparticles by Citrus limon (lemon) aqueous extract and theoretical prediction of particle size. Colloids and Surfaces B: Biointerfaces, 82(1), 152-159

29. Ramnami, S.P., J. Biswal and S. Sabharwal 2007. Synthesis of silver nanoparticles supported on silica aerogel using gamma radiolysis. Radiat Phys Chem, 76:1290-1294.

30. Reddy, A.S.; C.Y. Chen, S.C. Baker, C.C. Chen, J.C. Jean, C.W. Fan, H.R. Chen and J.C. Wang 2009. Synthesis of silver nanoparticles using surfactin: A biosurfactant as stabilizing agent. Mater. Lett. 63, 1227–1230

31. Rodrigues, L., I. M. Banat, J. Teixeira, and R. Oliveira 2006. Biosurfactants: potential applications in medicine. Journal of Antimicrobial Chemotherapy, 57(4), 609-618

32. Santa Anna, L. M., G. V. Sebastian, E. P. Menezes, T. L. M. Alves, A. S. Santos, N.Pereira Jr and Freire, D. M. G. 2002. Production of biosurfactants from Pseudomonas aeruginosa PA 1 isolated in oil environments. Brazilian Journal of Chemical Engineering, 19(2), 159-166

33. Seil, J. T. and T. J. Webster 2012. Antimicrobial applications of nanotechnology: methods and literature. International Journal of Nanomedicine, 7, 2767

34. Shaban, S. M. 2016. Studying the effect of newly synthesized cationic surfactant on silver nanoparticles formation and their biological activity. Journal of Molecular Liquids, 216, 137-145

35. Shaban, S. M., I. Aiad, M. M. El-Sukkary, E. A. Soliman and M. Y. El-Awady 2015. Preparation of capped silver nanoparticles using sunlight and cationic surfactants and their biological activity. Chinese Chemical Letters, 26(11), 1415-1420

36. Shekhar, S., A. Sundaramanickam and T. Balasubramanian 2015. Biosurfactant producing microbes and their potential applications: a review. Critical Reviews in Environmental Science and Technology, 45(14), 1522-1554

37. Sheppard, J. D. and C. N. Mulligan 1987. The production of surfactin by Bacillus subtilis grown on peat hydrolysate. Applied Microbiology and Biotechnology, 27(2), 110-116

38. Smyth, T. J. P., A. Perfumo, S. McClean, R. Marchant and I. M. Banat 2010. Isolation and analysis of lipopeptides and high molecular weight biosurfactants. Handbook of hydrocarbon and lipid microbiology, pp:3687-3704

39. Sobczak-Kupiec, A., D. Malina, Z. Wzorek and M. Zimowska 2011. Influence of silver nitrate concentration on the properties of silver nanoparticles. Micro & Nano Letters, 6(8), 656-660

40. Song K.C., S.M. Lee, T.S. Park and B.S. Lee 2009. 'Preparation of colloidal silver nanoparticles by chemical reduction method', Korean J. Chem. Eng., , 26, pp. 153 –155

41. Stensberg, M. C., Q. Wei, E. S. McLamore, D. M., Porterfield, A. Wei, and M. S. Sepúlveda 2011.Toxicological studies on silver nanoparticles: challenges and opportunities in assessment, monitoring and imaging. Nanomedicine, 6(5), 879-898

42. Velammal, S. P., T. A. Devi and T. P. Amaladhas 2016. Antioxidant, antimicrobial and cytotoxic activities of silver and gold nanoparticles synthesized using Plumbago zeylanica bark. Journal of Nanostructure in Chemistry, 6(3), 247-260

43. Velgosová, O., A. Mražíková and R. Marcinčáková 2016. Influence of pH on green synthesis of Ag nanoparticles. Materials letters, 180, 336-339

44. Wang, H., H. Wang, T. Li, J. Ma, K. Li, and X. Zuo 2017. Silver nanoparticles selectively deposited on graphene-colloidal carbon sphere composites and their application for hydrogen peroxide sensing. Sensors and Actuators B: Chemical, 239, 1205-1212

45. Yalcin, E. and A. Ergene 2009. Screening the antimicrobial activity of biosurfactant produced by microorganisms isolated from refinery wastewaters. J. Appl. Biolog. Sci. 3(2): 148-153

46. Yusof, F., S. Chowdhury, N. Sulaiman and M. O. Faruck, 2018. Effect of process parameters on the synthesis of silver nanoparticles and its effects on microbes. Jurnal Teknologi, 80(3).

47. Zhang, J., M. Chaker and D. Ma 2017. Pulsed laser ablation based synthesis of colloidal metal nanoparticles for catalytic applications. Journal of Colloid and Interface Science, 489, 138-149

48. Zhao, X., L. Zhou, M. S. Riaz Rajoka, L. Yan, C. Jiang, D. Shao and M. Jin 2018. Fungal silver nanoparticles: synthesis, application and challenges. Critical Reviews in Biotechnology, 38(6), 817-835.

.